Structural and Chemical Investigations of $Na_3(ABO_4)_3 \cdot 4H_2O$-Type Sodalite Phases

Tina M. Nenoff,[†,‡] William T. A. Harrison,[§] Thurman E. Gier,[†] Nancy L. Keder,[†] Charlotte M. Zaremba,[†] Vojislav I. Srdanov,[†] Jaqueline M. Nicol,[∥] and Galen D. Stucky*[,†]

Department of Chemistry, University of California, Santa Barbara, California 93106-9510, Department of Chemistry, University of Houston, Houston, Texas 77204-5641, and Reactor Radiation Division, National Institute of Standards and Technology, Gaithersburg, Maryland 20899-0001

Received December 15, 1993[⊗]

The sodalite cage containing only an electron as a nonframework "anion" is well adapted for the study of solvated "electride" Wigner lattices and quantitative mapping of the intra- and intercage electronic potential surfaces. In this paper we report the direct synthesis of anion free cage structures of the form $Na_3[\,](ABO_4)_3 \cdot nH_2O$ (A; B = Al, Ga; Si, Ge) as possible precursors for sodalite electride synthesis. A novel, low-temperature sodalite dehydroxylation method is presented for the preparation of $Na_3[\,](AlSiO_4)_3 \cdot 4H_2O$ from $Na_4[OH](AlSiO_4)_3 \cdot 1.72H_2O$. Results from a neutron diffraction study of $Na_3(ZnAsO_4)_3 \cdot 4H_2O$ give evidence of hydrogen bonding between the framework oxygen atoms and the β-cage substructure and aid in explanation of analog unit cell trends. All of the investigated sodalites have an ordered array of their framework tetrahedral cations and crystallize in the cubic space group $P\bar{4}3n$, $Z = 2$. Two of these new sodalites were characterized by single-crystal X-ray diffraction. $Na_3(AlGeO_4)_3 \cdot 4H_2O$, with $a = 8.965(1)$ Å, d(Al–O) = 1.746(4) Å, d(Ge–O) = 1.758(4) Å, and Θ(Al–O–Ge) = 129.6(2)°, has β-cages which contain a defect-"cubane"-like $Na_3 \cdot 4H_2O$ array. Final disagreement factors: $R = 1.93\%$ and $R_w = 2.19\%$ for 208 observed reflections [$I > 3\sigma(I)$]. $Na_3(GaGeO_4)_3 \cdot 4H_2O$, with $a = 9.0033(7)$ Å, d(Ga–O) = 1.839(3) Å, d(Ge–O) = 1.745(3) Å, and Θ(Ga–O–Ge) = 125.3(2)°, has the same β-cage contents. Final disagreement factors of $R = 1.00\%$ and $R_w = 1.29\%$ were obtained for 183 observed reflections [$I > 3\sigma(I)$]. The structure of $Na_3[(GaSiO_4)_3] \cdot 4H_2O$ was determined by Rietveld refinement of room-temperature X-ray powder diffraction data, with $a = 8.8614(2)$ Å, d(Ga–O) = 1.847(4) Å, d(Si–O) = 1.580(3) Å, Θ(Ga–O–Si) = 131.9(3)°, and the same β-cage contents. Final disagreement factors of $R_p = 10.07\%$ and $R_{wp} = 13.75\%$ for 4099 data were obtained. The structure of $Na_3(ZnAsO_4)_3 \cdot 4H_2O$ was determined from low-temperature continuous-wavelength neutron powder diffraction data, with $a = 9.0276(7)$ Å, d(Zn–O) = 1.974(4) Å, d(As–O) = 1.689(4) Å, Θ(Zn–O–As) = 121.1(3)°, and the same β-cage contents, with evidence of hydrogen bonding between cubane and framework atoms. Final disagreement factors of $R_p = 4.26\%$ and $R_{wp} = 5.52\%$ for 3268 data were obtained. These isomorphs are compared with other $Na_3[\,](ABO_4)_3 \cdot 4H_2O$ types of sodalite structures in terms of geometrical trends in 6-ring topologies and cation and water molecule sitings. Further structural information is obtained through presented spectral, thermogravimetric, and physical data.

Introduction

Sodalite, $Na_4Cl(AlSiO_4)_3$,[1] is the type-species for a large family of related aluminosilicate structures of general formula $M_{4-x}X_{1-x}(AlSiO_4)_3 \cdot (4-y)H_2O$ (M = univalent cation; X = univalent anion). The relationship between the allowed values of x and y has been discussed previously for the aluminosilicate framework.[2] The crystal structure of sodalite (Figure 1) is built up from tetrahedral building blocks (*e.g.*, SiO_4 and AlO_4), linked together to form a truncated octahedral β-cage, containing eight 6-ring openings and six 4-ring opernings.[3] The cage diameter is about 6.5 Å, and the 6- and 4-rings have a free diameter of about 2.2 and 1.6 Å, respectively, depending on the precise species involved. In sodalite, the β-cages are built into a close-packed array, and the sodalite β-cage also occurs as a building block in other zeolite species such as faujasite and hexagonal-faujasite.

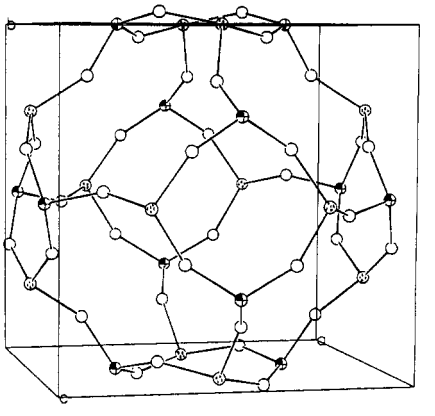

Figure 1. ORTEP[31] figure of the generic sodalite framework cage, with dotted and shaded atoms representing the different T-atoms and plain atoms as oxygen atoms (without the intercage sodium/water cluster).

Most sodalite tetrahedral-framework lattices contain a formal negative charge, which is balanced by extra-framework cations, typically located in the 6-ring β-cage windows, for example, $Na_3(AlSiO_4)_3$.[2] The sodalite framework is atypical in also admitting extra-framework *anions* into the structure, which are charge balanced by additional extra-framework *cations*, *e.g.*, $Na_4(OH)(AlSiO_4)_3$ (or $Na_3(AlSiO_4)_3 \cdot NaOH$).[2,4,5] In addition, up to four water molecules per sodalite β-cage may or may not be included

* Author for correspondence.
† University of California.
‡ Current address: Sandia National Laboratories, P.O. Box 5800, Org. 6212, MS 0709, Albuquerque, NM 87185-0709.
§ University of Houston.
∥ National Institute of Standards and Technology. Disclaimer: Certain trade names and company products are mentioned in the text or identified in an illustration in order to adequately specify the experimental procedure and equipment used. In no case does such identification imply recommendation or endorsement by the National Institute of Standards and Technology, nor does it imply that the products are necessarily the best available for the purpose.

⊗ Abstract published in *Advance ACS Abstracts,* April 15, 1994.

(1) Pauling, L. *Z. Kristallogr.* **1930**, *74*, 213.
(2) Barrer, R. M.; Cole, J. F. *J. Chem. Soc. A* **1970**, 1516.
(3) Breck, D. W. *Zeolite Molecular Sieves*; Krieger Publishing Co.: Malabar, FL, 1984.
(4) Hassan, I.; Grundy, H. D. *Acta Crystallogr.* **1983**, *C39*, 3.

0020-1669/94/1333-2472$04.50/0

Table 1. Sodalite Structural Data

framework	space group	q^a	comments
$(SiO_2)_6{\cdot}C_2H_4(OH)_2$	$Im\bar{3}m$	0	silica sodalite[b,c]
$AlPO_4{\cdot}nN(CH_3)_4(OH)$	$P\bar{4}3n$	0	AlPO-20
$Na_4Cl(AlSiO_4)_3$	$P\bar{4}3n$	−3	chloro–sodalite
$Na_4I(AlSiO_4)_3$	$Pm\bar{3}n$	−3	high-temp iodo–sodalite[b]
$Na_3(AlSiO_4)_3{\cdot}4H_2O$	$P\bar{4}3n$	−3	hydrated sodalite
$Na_4OH(AlSiO_4)_3{\cdot}2H_2O$	$P\bar{4}3n$	−3	hydrated basic sodalite
$Na_4OH(AlSiO_4)_3{\cdot}2H_2O$	$P222$	−3	low-temp hydrated basic sodalite
$Na_3(ZnPO_4)_3$	$P\bar{4}3n$	−3	zincophosphate sodalite
$Li_4Br(BePO_4)_3$	$P\bar{4}3n$	−3	beryllophosphate sodalite
$Na_4Cl(AlBeSi_4O_{12})$	$I\bar{4}$	−3	tugtupite[d]
$Ca_4(OH)_4(Al_2SiO_6)_2$	$I\bar{4}3m$	−4	bicchulite[c]
$Sr_4MoO_4(AlO_2)_6$	$I4_1/acd$	−6	low-temp aluminate sodalite[c]
$Sr_4MoO_4(AlO_2)_6$	$Im\bar{3}m$	−6	high-temp aluminate sodalite[b,c]
$Zn_4S(BO_2)_6$	$I\bar{4}3m$	−6	zinc sulfide boralite[c]
$(Ga_3Zn)P(BO_2)_6$	$I\bar{4}3m$	−6	zinc/gallium phosphide boralite[c]
$Cd_4S(BeSiO_4)_3$	$P\bar{4}3n$	−6	cadmium sulfide helvite

[a] q = formula-unit framework charge. [b] Fully-expanded framework. [c] Disordered/uniatomic framework. [d] 3-Ordered framework cations.

in the structure, and a very large variety of sodalite-type structures are known. A nonexclusive list of guest species includes Na^+, K^+, Li^+, and Ag^+ as cations and Cl^-, Br^-, I^-, OH^-, NO_3^-, NO_2^-, *etc.*, as anions. Additionally, the aluminum:sodium ratio may differ from 1:1, and sodalites with pure alumina and pure silica frameworks are known: the former requires divalent extra-framework cations for charge balance,[6] while the latter is neutral.[7]

Sodalites are on the borderline between "open" zeolitic and condensed aluminosilicate structures, as they contain a close-packed array of small cages, only interlinked via relatively small 6-rings.[3] However, typical zeolitic reactions are possible: sodalites have been shown to undergo (cationic) ion-exchange reactions, subject to the typical size restrictions imposed by the 6-ring intercavity windows. The facile exchange of silver for sodium has been rationalized in terms of hard/soft-acid/base interactions. Reversible dehydration/hydration and its dramatic effect on framework geometry has also been demonstrated.[8] Many non-aluminosilicate sodalite analogs have been prepared: compared with the ABO_4 framework formula unit $Al_{1+x}Si_{1-x}O_4$ ($-1 \le x \le 1$) other sodalite-types corresponding to B_2O_4, $BePO_4$, $BeAsO_4$, $Ga_{1-z}Si_{1+z}O_4$ ($-0.01 \le z \le 0.168$),[9] $AlGeO_4$,[10,11] $BeGeO_4$, $BeSiO_4$, $ZnPO_4$, $ZnAsO_4$, and other framework-atom configurations are known. Some sodalite data are listed in Table 1.[12]

Recently our interests have focused on the optical and electronic properties of the inorganic "electride" sodalite analogs $M_4[e^-](AlSiO_4)_3$ (M = monovalent metal atom) which can be envisioned as a Wigner lattice of electrons modulated by the sodalite framework potential surface.[13,14] The unpaired electron interactions with the sodalite cage walls and with electrons in adjacent cages provides an opportunity to study the intra- and intercage potential. The cage geometry can be varied for a given framework composition by using different cations (M) and various combinations of different monovalent cations (i.e. M_4, M_{4-n}) or by varying the electron anion ($[X^-]$) occupancy as in $M_4[e^-]_{1-y}[X^-]_y(AlSiO_4)_3$. An alternative approach to controlling the electronic potential properties is to synthesize zeolite analog structures with different framework atoms. Such structures are well-known for compositions of the form $M_4[X][ABO_4]_3{\cdot}nH_2O$, where X is an anion (e.g. OH^- halide or oxo anion) and A, B are elements from groups 2 and 13–15. Examples include structure compositions B_2O_4, $BePO_4$, $BeAsO_4$, $AlPO_4$, $Ga_{1-z}Si_{1+z}O_4$, $AlGeO_4$, $BeGeO_4$, $BeSi_4$, $ZnPO_4$, $ZnAs_4$, and Al_2O_4. Our interest is in the empty (anion free) cage of the form $M_3[\ ](ABO_4)_3$ which can then be appropriately filled by vapor-phase deposition with electron donors and/or acceptors to form small charge carrier clusters.

Crystallographically, sodalites may be described in various space groups, depending on the ordering of the tetrahedral cations and degree of "folding"[15] of the framework, to accommodate the guest species. The ideal, fully-expanded lattice belongs to space group $Im\bar{3}m$; the folded variant of this disordered tetrahedral lattice crystallizes as $I\bar{4}3m$. For an ordered array of tetrahedral cations, $Pm\bar{3}n$ is the space group describing the fully-expanded lattice, or $P\bar{4}3n$ for the folded lattice. Various noncubic unit cells have also been observed in sodalite-types. This folding is crucial in defining the window sizes and extra-framework geometries, as discussed further below. Sodalites of the formula $Na_3(AlSiO_4)_3{\cdot}4H_2O$, and space group $P\bar{4}3n$ follow the model put forth by Felsche et al., with the sodium cations and water molecules forming a defect-"cubane"-structure of $Na_3{\cdot}4OH_2$ in the cage.[16]

In this paper we describe the synthetic procedures used to synthesize numerous sodalite analogs (1) by the direct synthesis of "empty" cage precursors and (2) by a new low-temperature approach for removing hydroxyl groups from $Na_4[OH](AlSiO_4)_3{\cdot}nH_2O$. The examples we describe of the three analogs of the hydrated sodium aluminosilicate sodalite ($Na_3[\ ](AlSiO_4)_3{\cdot}4H_2O$) phase contain aluminum and germanium ($Na_3(AlGeO_4)_3{\cdot}4H_2O$: AlGe–SOD), gallium and germanium ($Na_3(GaGeO_4)_3{\cdot}4H_2O$: GaGe–SOD), and gallium and silicon ($Na_3(GaSiO_4)_3{\cdot}4H_2O$: GaSi–SOD) as the framework tetrahedral atoms (T-atoms). We also examine the hydrogen bonding between the framework oxygen atoms and the β-cage cubane water protons in the $Na_3(ZnAsO_4)_3{\cdot}4H_2O$ (ZnAs–SOD) analog. High-quality crystallographic data for these phases are compared with other $Na_3(ABO_4)_3{\cdot}4H_2O$-type sodalites, and trends in framework geometry, extra-framework sites, and physical properties are examined, along with observations concerning the electronic potentials of nonaluminosilicate frameworks.

Experimental Section

Synthesis. $Na_3(AlGeO_4)_3{\cdot}4H_2O$ was synthesized by the mixing of 17.22 g of 0.75 M Na_4GeO_4 (11 mmol) and 3.44 g of 4 M $Na_2Al_6O_2OH$ (10 mmol) in a polypropylene bottle and then the slow addition of 2.16 g of concentrated (70%) HNO_3 (24 mmol). The initial gel precipitate redissolved readily. However, after holding at 70 °C for 2 weeks, masses of small crystals had formed and were recovered for structure determination.

$Na_3(GaGeO_4)_3{\cdot}4H_2O$ was synthesized by mixing 30.98 g of 0.8 M Na_4GeO_4 (20 mmol) and 17.64 g of 2 M Na_5GaO_4 (24 mmol) in a polypropylene bottle. The clear solution was partially neutralized by the addition of 12.96 g of concentrated (70%) HNO_3 (144 mmol). During the slow acid addition, a gel precipitated but redissolved on agitation. The final clear solution was held at 100 °C for 4 days, during which time cubic crystals up to 0.4 mm slowly grew on the container walls.

$Na_3(GaSiO_4)_3{\cdot}4H_2O$ was synthesized by mixing 17.6 g of 2 M Na_5GaO_4 (24 mmol), 15.35 g of 2 M Na_2SiO_3 (25 mmol), and 20 mL of H_2O in a polypropylene bottle. To this clear solution was added 8.69 g of concentrated (70%) HNO_3 (96.5 mmol). The initial gel redissolved on agitation, and the clear solution was allowed to crystallize at 100 °C for 3 days. A 15% yield contained 0.75 g of minicrystals.

(5) Engelhardt, G.; Felsche, J.; Sieger, P. *J. Am. Chem. Soc.* **1992**, *114*, 1173.
(6) Depmeier, W. *Acta Crystallogr.* **1984**, *C40*, 226.
(7) Bibby, D. M.; Dale, M. P. *Nature* **1985**, *317*, 157.
(8) Nenoff, T. M.; Harrison; W. T. A., Stucky, G. D.; Newsam, J. M. *Zeolites* **1993**, *13* (7), 506.
(9) Newsam, J. M.; Jorgensen, J. D. *Zeolites* **1987**, *7*, 569.
(10) Uvarova, T. G.; Dem'yanets, L. N.; Lobachev, A. N. *Sov. Phys. Crystallogr.* **1976**, *21* (4), 497.
(11) Fleet, M. E. *Acta Crystallogr.* **1989**, *C45*, 843.
(12) Meier, W. M.; Olson, D. H. *Atlas of Zeolite Structure Types*; Polycrystal Book Service: Pittsburgh, PA, 1978.
(13) Srdanov, V. I.; Haug, K.; Metiu, H.; Stucky, G. D. *J. Phys. Chem.* **1992**, *96*, 9039.
(14) Haug, K.; Srdanov, V. I.; Stucky, G. D.; Metiu, H. *J. Chem. Phys.* **1992**, *96*, 3495.
(15) Depmeier, W. *Z. Kristallogr.* **1992**, *199*, 75.
(16) Felsche, J.; Luger, S.; Baerlocher, C. *Zeolites* **1986**, *6*, 367.

A fast, room-temperature two-step method of converting hydroxy hydrated sodium aluminosilicate sodalite to the hydrated phase was devised to replace the 48-h Soxhlet extraction method and make this reaction kinetically feasible for large single crystals.

The first step was to synthesize $Na_4(OH)(AlSiO_4)_3 \cdot 1.72H_2O$ powder by mixing 26.42 g of LUDOX colloidal SiO_2 (31%), 16.24 g of NaOH pellets, and 50.00 g of water in a Teflon bottle until the solution clarified, followed by the addition of 46.02 g of 4 M Na_2AlO_2OH. The gelatinous precipitate was shaken well (15 min), held for 4 days, filtered, and rinsed thoroughly with water and acetone, and then dried at 100 °C for 1 day. The final yield was 21.22 g. Powder X-ray diffraction revealed a primitive cubic unit cell with a = 8.8957(4) Å.

In the second step of the synthesis, 5 g of $Na_4(OH)(AlSiO_4)_3 \cdot 1.72H_2O$ was stirred in 100 mL of H_2O until the pH stabilized at 10.7 (basic because of NaOH expelled from the β-cages). To this basic solution, an equal number of moles of acid to moles of β-cage OH was added with constant monitoring of pH with an electronic pH meter. Acid was added slowly enough to prevent the pH from falling below 5.5, a condition which could cause hydrolysis of the framework.

Within 1 h, all β-cage OH^- groups were neutralized by the equimolar amount of acid. The material was filtered, rinsed, and dried immediately thereafter. Powder X-ray diffraction revealed a primitive cubic unit cell with a = 8.8465(9) Å, indicating the hydrated phase.

The 2 to 3 mm-sized crystals of hydroxy hydrated sodium aluminosilicate sodalite (hydrothermally synthesized in sealed gold tubes) were partially converted to the hydrated phase by suspension in 12.7 m sodium acetate buffered to pH 4.5 by addition of acetic acid and held at 80 °C for 3 weeks. These conditions increased the rate of NaOH extraction and then, once completed, protected the hydrated β-cages from protonation of intracage H_2O accompanied by loss of Na^+ and collapse of the framework structure. This treatment resulted in conversion to a poorly characterized, noncubic hydrated sodium aluminosilicate phase on the outer surfaces of the crystals[17] and a change in optical properties from clear to opaque, chalky white. Powder X-ray diffraction revealed that the remaining crystalline sodalite phase had a primitive cubic unit cell with a = 8.8419(8) Å, indicating the hydrated phase.

$Na_3(ZnAsO_4)_3 \cdot 4H_2O$ was synthesized by following procedures described earlier.[18]

Thermogravimetric Analysis. Thermogravimetric analysis data were initially collected on a DuPont 9900 system in air. Subsequent TGA and DSC studies were performed on a Netzsch Simultaneous Thermal Analysis (STA) 409 system under vacuum (0.005 mbar). The heating rate for both systems was 10 °C/min from room temperature to 900 °C.

Initial X-ray Diffraction Studies. A Scintag PAD-X automated diffractometer operating in θ–θ geometry was used at room temperature (25(1) °C). The instrumental $K\alpha_1/K\alpha_2$ profile was reduced to a single Cu $K\alpha_1$ peak position (λ = 1.540 568 Å) by a stripping routine, and d-spacings were established using silicon powder (a = 5.430 35 Å) as an internal standard, relative to this wavelength. Lattice parameters were optimized by least-squares refinements using Scintag software routines.

***In Situ* X-ray Diffraction Studies.** A Bühler HDK 2.3 high-temperature X-ray chamber and a Micristar control system were used with the Scintag PAD-X automated diffractometer. A sample, thoroughly mixed with a silicon standard, was loaded onto the temperature stage, and a diffraction pattern was collected. The rest of the experiment was performed on the same sample while under the constant evacuation of 1×10^{-6} Torr. At each stage, the temperature was raised immediately to the set point and equilibrated for 30 min, allowing for any water in the sample to be removed. The stepwise dehydration could be followed by the initial increase and then return to "normal" of the evacuated chamber pressure.

Second Harmonic Generation Measurements. Measurements of second harmonic generation (SHG) were performed on powder samples. The magnitudes of nonlinear optical coefficients were measured relative to crystalline quartz and presented as averaged waveforms (results of 1000 pulses). The experimental configuration was similar to that of Kurtz and Perry[19] except for the use of a ≈10 mJ/pulse from 1.064-μm probe radiation, generated by a Q-switched Nd-Yag laser (Quanta Ray-DCR-11) operating at 10 Hz. The well-ground crystalline powder was compacted inside the melting probe capillary on which the input beam was softly focused. A small monochromator, tuned at 532 nm, was used as a band pass filter to eliminate any spurious light possibly present during the experiment.

Table 2. Crystallographic Parameters for $Na_3(AlGeO_4)_3 \cdot 4H_2O$

emp formula	$Ge_3Al_3Na_3O_{16}H_8$	fw	631.73
a	8.965(1) Å	space group	$P\bar{4}3n$ (No. 218)
b	8.965(1) Å	λ(Mo Kα)	0.710 73 Å
c	8.965(1) Å	ρ_{calc}	2.875 g cm^{-3}
V	720.40 Å^3	μ	64.88 cm^{-1}
Z	2	$R(F)$	1.93%
T	25(2) °C	$R_w(F)^b$	2.19%

^{a} $R = \sum||F_o| - |F_c||/\sum|F_o|$. ^{b} $R_w = [\sum w(|F_o| - |F_c|)^2/\sum w|F_o|^2]^{1/2}$.

Crystallographic Data

For $Na_3(AlGeO_4)_3 \cdot 4H_2O$, a suitable cube-like single crystal (edge dimension approximately 0.15 mm) for structure determination was selected and mounted on a thin glass fiber with cyanoacrylate glue. Room-temperature (25(2) °C) intensity data were collected on a Huber automated 4-circle diffractometer (graphite-monochromated Mo Kα radiation, λ = 0.710 73 Å) as outlined in Table 2. A total of 25 reflections were located and centered by searching reciprocal space and indexed to obtain a unit cell and orientation matrix. The cubic unit cell constant was optimized by least-squares refinement, resulting in a value of a = 8.965(1) Å. Intensity data were collected in the θ–2θ scanning mode with standard reflections monitored for intensity variation throughout the course of each experiment. The scan speed was 6°/min with a scan range of 1.3° below $K\alpha_1$ to 1.6° above $K\alpha_2$. No significant variation in standards was observed, and crystal absorption was empirically corrected for using ψ-scans through 360° for selected reflections, but no absorption correction was applied. The raw data were reduced to F and $\sigma(F)$ values by using a Lehmann–Larsen profile-fitting routine, and the normal corrections for Lorentz and polarization effects were made. All the data collection and reduction routines were based on the UCLA crystallographic computing package. The systematic absences (hhl, l and 00l, l) in the reduced data were consistent with space groups $P\bar{4}3n$ and $Pm\bar{3}n$. A second harmonic generation (SHG) test[19] yielded a value 2.4 times quartz, indicating the noncentrosymmetric space group, $P\bar{4}3n$.

The initial values for the framework-atom coordinates (Al, Ge, O(1)) in space group $P\bar{4}3n$ were taken from the ZnAs– and ZnP–SOD structures: these models assumed an ordered, alternating array of AlO_4 and GeO_4 tetrahedra in a 1:1 ratio.[18] After refinement of the framework atomic positional, and thermal factors, the extra-framework species were located by difference Fourier syntheses. Two prominent x, x, x-type peaks on the cubic body diagonal were observable: a site ≈ 0.15, 0.15, 0.15, and one ≈0.38, 0.38, 0.38. These were assigned to sodium (occupancy = 0.75) and oxygen (water molecule, occupancy = 1.0) atoms, respectively, by analogy with previous studies on other sodalite-type phases.[18] There was no significant residual electron density at the origin of the unit cell, a site typically occupied by an anionic species in $M_4X(AlSiO_4)_3$ sodalites. The positions, thermal factors, and occupancies of the guests were added to the refinement, which converged satisfactorily to the final disagreement indices indicated below.

The least-squares and subsidiary calculations were performed using the Oxford CRYSTALS[20] system, running on a DEC μVAX-II computer. Final full-matrix refinements were against F and included anisotropic temperature factors and a secondary extinction correction[21] (refined value = 56(3)). Complex, neutral-atom scattering factors were obtained from ref 22. Final disagreement values, defined in Table 2: R = 1.93%, R_w = 2.19% (21 parameters, 208 observed reflections with $I > 3\sigma(I)$). Final Fourier difference maps revealed no regions of significant electron density, and analysis of the various trends in F_o versus F_c revealed no unusual effects.

For the $Na_3(GaGeO_4)_3 \cdot 4H_2O$ system, room-temperature powder X-ray diffraction results indicated a primitive cubic crystal system with a = 9.000(5) Å. However, preliminary single-crystal X-ray scans indicated a body-centered cubic unit cell, as found for sodalites containing a disordered tetrahedral-atom array, and a structural model was successfully refined in space group $I\bar{4}3m$ to excellent agreement indices (*vide infra*).

(17) Sazhin, V. S.; Pankeeva, E. T. *Sov. Prog. Chem.* **1971**, *37* (2), 43.
(18) Nenoff, T. M.; Harrison, W. T. A.; Gier, T. E.; Stucky, G. D. *J. Am. Chem. Soc.* **1991**, *113*, 378.
(19) Kurtz, S. K.; Perry, T. T. *J. Appl. Phys.* **1968**, *39*, 3798.
(20) Watkin, D. J.; Carruthers, J. R.; Betteridge, P. W. *CRYSTALS User Guide*; Chemical Crystallography Laboratory: Oxford University, U.K., 1990.
(21) Larson, A. C. In *Crystallographic Computing*; Ahmed, F. R., Ed.; Munksgaard: Copenhagen, 1970.
(22) *International Tables for X-ray Crystallography*; International Union for Crystallography: Birmingham, U.K., 1974; Vol. IV.

Table 3. Crystallographic Parameters for $Na_3(GaGeO_4)_3{\cdot}4H_2O$

emp formula	$Ge_3Ga_3Na_3O_{16}H_8$	fw	759.95
a	9.0033(7) Å	space group	$P\bar{4}3n$ (No. 218)
b	9.0033(7) Å	λ(Mo Kα)	0.710 73 Å
c	9.0033(7) Å	ρ_{calc}	3.421 g cm^{-3}
V	729.79 Å^3	μ	116.34 cm^{-1}
Z	2	$R(F_o)^a$	1.00%
T	25(2) °C	$R_w(F_o)^b$	1.29%

[a] See Table 2 for definition of R. [b] $R_w = [\sum w(||F_o| - |F_c||)^2/\sum w|F_o|^2]^{1/2}$.

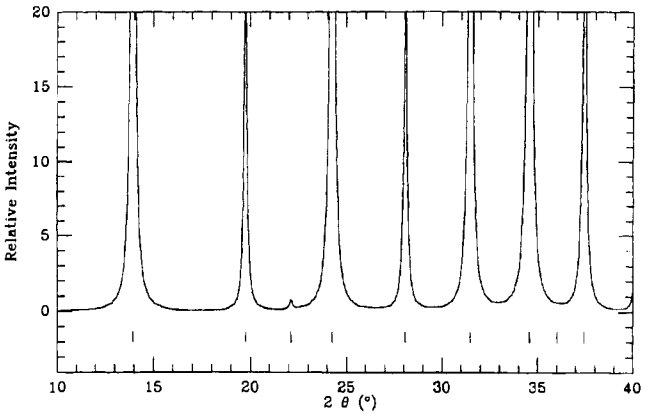

Figure 2. LAZY-PULVERIX[23] simulation of GaGe–SOD powder diffraction. Use of the single-crystal parameters confirmed the relative weakness of all the possible primitive reflections which violate the $h + k + l$ even body-centering condition.

Careful examination of X-ray powder data for $Na_3(GaGeO_4)_3{\cdot}4H_2O$ showed that the (012) reflection was weakly observable ($I_{rel}(012) \approx 5$ relative to $I_{max}(440) = 1000$), violating the body-centering condition. Slow single-crystal X-ray scans (scan speed = 1.5°/min) indicated that several primitive reflections were observable, with $I \geq 10\sigma(I)$: these $I/\sigma(I)$ ratios were consistent among equivalent reflections, indicating that these intensities were real. The data were recollected as primitive-cubic (Table 3) and then modeled as an ordered T-atom sodalite as described above for the aluminogermanate phase. A successful refinement in space group $P\bar{4}3n$ (extinction parameter = 111(8)) resulted in final disagreement values of R = 1.00% and R_w = 1.29% for 183 observed reflections with $I > 3\sigma(I)$. By comparison, the refinement in $I\bar{4}3m$ led to agreement factors of R = 1.26% and R_w = 1.42%. A LAZY-PULVERIX[23] simulation of the X-ray powder pattern of $Na_3(GaGeO_4)_3{\cdot}4H_2O$ using the single-crystal parameters obtained above confirmed the relative weakness of all the possible primitive reflections which violate the $h + k + l$ even body-centering condition (see Figure 2).

For $Na_3(GaSiO_4)_3{\cdot}4H_2O$, a combination of the initial (3°/min) room-temperature powder X-ray diffraction data and a SHG response of 2.4 times quartz was used to determine the noncentrosymmetric space group $P\bar{4}3n$ of the finely ground powder, with a cell edge of a = 8.861(4) Å. The structure determination process involved room-temperature (25(1) °C) data collection on the same diffractometer system, between 2θ = 18 and 100°, with a step size of 0.02° for a total of 4099 data. Rietveld refinement was carried out using the program GSAS. The crystal structure of this material was established by X-ray Rietveld refinement, using the starting sodium aluminogermanate model (from above) in space group $P\bar{4}3n$.[18] Assuming that the framework geometry remained the same, except for slight distortions to bond lengths and angles, coordinates were entered for strict alternation of GaO_4 and SiO_4 tetrahedra (T-atoms) in a 1:1 ratio. The profile R factor was over 20%, after the usual refinement of scale factor, detector zero-point correction, background coefficients, unit cell parameter, peak shape-width variation terms, and framework-atom positional and isotropic thermal parameters, but without any cation refinements. The sodium cation was placed at a (x, x, x) special position and with 75% occupancy, while the oxygen atoms of the included water molecules were placed at another (x, x, x) special position with 100% occupancy. Refinement of the sites and occupancies converged to x = 0.1461(6) and 75% and 0.3750(5) and 100%, respectively. Successive Fourier difference maps did not locate any other atomic sites

(23) Yvon, K.; Jeitschko, W.; Parthe, E. *LAZY-PULVERIX User Guide*; University of Geneva: Geneva, Switzerland, 1976.

Table 4. Crystallographic Parameters for $Na_3(GaSiO_4)_3{\cdot}4H_2O$

emp formula	$Ga_3Si_3Na_3O_{16}H_8$
mol wt	626.40
habit	white powder
cryst system	cubic
$a = b = c$	8.8614(2) Å
$\alpha = \beta = \gamma$	90°
V_{calc}	695.84 Å^3
Z	2
space group	$P\bar{4}3n$
T	25(2) °C
no. of λ(Cu Kα)	1.5406 Å
refinement method	X-ray Rietveld refinement
peak shape function	pseudo-Voigt
data range	$20 \leq 2\theta \leq 100°$
no. of data	4099 powder data points
no. of params	25
$R_p{}^a$	10.07%
$R_{wp}{}^b$	13.76%

[a] $R_p = \sum|y_o - Cy_c|/\sum|y_o|$. [b] $R_{wp} = [\sum w(|y_o - Cy_c|)^2/\sum w|y_o|^2]^{1/2}$. C is a scale factor.

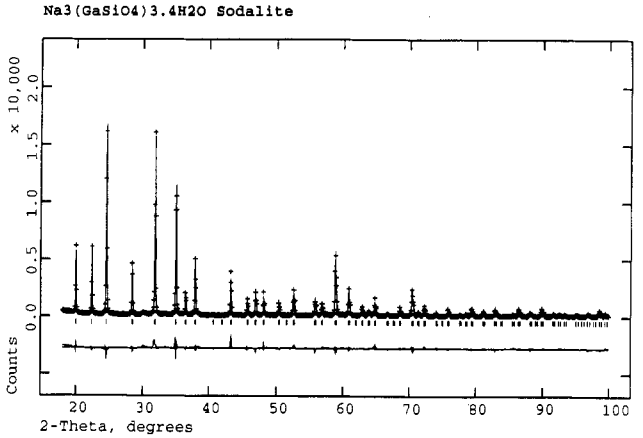

Figure 3. Final observed, calculated, and difference profiles of GaSi–SOD room-temperature powder X-ray diffraction data.

in the sodalite cage. As a further test on the possibility of it having a similar structure with basic sodalite,[2,4,5] OH^- was separately placed (during different refinement cycles) at the origin and refined. No convergence was obtained when occupancies were fixed to 100%, and the R factor increased dramatically. The final cycle of least squares converged to give residuals of R_p = 10.07% and R_{wp} = 13.76% (χ^2 = 7.79) for 25 variables (see Table 4). The final observed, calculated, and difference profiles are illustrated in Figure 3.

For $Na_3(ZnAsO_4)_3{\cdot}4H_2O$, low-temperature continuous-wavelength neutron data were collected and refined using the same parameters from previously refined room-temperature X-ray data, in space group $P\bar{4}3n$ with a cell edge of a = 9.027 Å.[15] The structure determination process on this hydrated system involved low temperature, constant-wavelength powder neutron diffraction. Measurements were taken on the high-resolution, five-detector, powder diffractometer on beam line BT-1, at the NBSR, National Institute of Standards and Technology (NIST), Gaithersburg, MD. The 5-gram sample was loaded in an air-free drybox into a 1-cm diameter cylindrical vanadium can and capped with indium-sealed titanium ends. The data were collected at 14(1) K, using a neutron wavelength of 1.553 Å, between 2θ = 5 and 120°, with a step size of 0.05°. Prior to analysis, the data were corrected for detector effects and collated. The Rietveld profile refinement was carried out with the program GSAS.[24] The profile R factor was slightly over 6%, after the usual refinement of scale factor, detector zero-point corrections, background coefficients, unit cell parameter, peak shape-width variation terms, and all framework and cation atom positional and isotropic thermal parameters, but without any proton refinements. The sodium cation was placed in at a (x, x, x) special position and with 75% occupancy, while the oxygen of the included water molecules were placed at another (x, x, x) special position with 100% occupancy. Refinement of the sites and occupancies converged to x = 0.137(2) and 75% and 0.3739(7) and 100%, respectively.

(24) Larson, A. C.; Von Dreele, R. B. *GSAS User Guide*; Los Alamos National Laboratory: Los Alamos, NM 87545, 1985–1988.

Table 5. Crystallographic Parameters for $Na_3(ZnAsO_4)_3{\cdot}4H_2O$

emp formula	$As_3Zn_3Na_3O_{20}H_8$
mol wt	818.20
habit	white powder
cryst system	cubic
$a = b = c$	9.0276(7) Å
$\alpha = \beta = \gamma$	90°
V_{calc}	735.73(3) Å^3
Z	2
space group	$P\bar{4}3n$
T	14(1) °C
λ(neutrons)	1.553 Å
refinement method	constant-wavelength Rietveld refinement
software	GSAS suite
peak shape function	Gaussian
data range	$5 \le 2\theta \le 120°$
no. of data	3268 powder data points
no. of params	45
R_p[a]	4.26%
R_{wp}[b]	5.52%

[a] $R_p = \sum|y_o - Cy_c|/\sum|y_o|$. [b] $R_{wp} = [\sum w(|y_o - Cy_c|)^2/\sum w|y_o|^2]^{1/2}$. C is a scale factor.

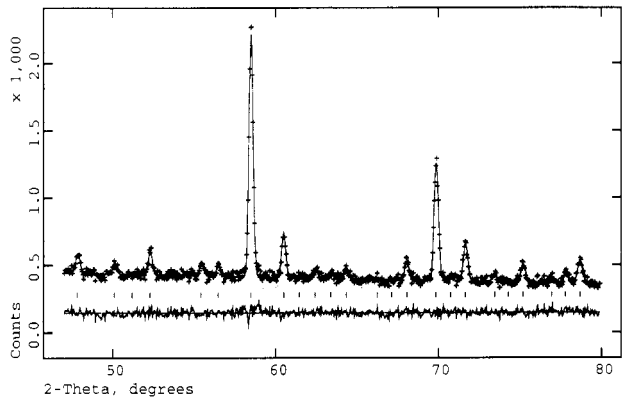

Figure 4. Final observed, calculated, and difference Rietveld profile plots for detector bank #3 ($47° < 2\theta < 80°$) for the ZnAs–SOD powder neutron refinement. The signal to noise ratio of the data is surprisingly good, considering the hydrogenous sample employed.

Protons were inputted at coordinates determined by negative peaks located in successive Fourier difference. However, refinements produced improbably short oxygen–hydrogen bond lengths. Following a model for proton locations from the AlSi–SOD,[25] each atom was placed on a (x, y, z) position near $^1/_3$ and at $^1/_3$ fixed occupancy. The final cycle of least squares converged to give residuals of $R_p = 4.26\%$ and $R_{wp} = 5.52\%$ ($\chi^2 = 1.379$) for 45 variables (see Table 5). The final observed, calculated, and difference profiles are illustrated in Figure 4.

Discussion

The sodalite type-species offers many facets of study in both the electronic potential of the surface based on the selection of atoms used for the tetrahedral connectivity and also the occupants of the cage. Earlier work on $Na_3[\ ](AlSiO_4)_3{\cdot}4H_2O$ has determined the crystal structure of the framework and the "cubane"-type substructure of $Na_3{\cdot}4OH_2$ that occupies the β-cage. Further studies have shown that this material can be loaded with a nonframework anion and studied as a solvated "electride" Wigner lattice.[13,14] In an effort to synthesize larger unit cells and pore openings in the sodalite framework system, we have attempted to incorporate a wide range of group III/IV atoms in combinations from very small (Al/Si) to very large (Zn/As) T-atom radii. Results have shown that these frameworks are not confined solely to aluminum and silicon but can be easily synthesized as analogs containing A = Al, Ga or Zn and B = Si, Ge, As, or P[17] in the $Na_3[\ ](ABO_4)_3{\cdot}4H_2O$ structure.

(25) Felsche, J.; Luger, S.; Fischer, P. *Acta Crystallogr.* **1987**, *C43*, 809.

Table 6. Atomic Positional Parameters and U_{eq} Values for $Na_3(AlGeO_4)_3{\cdot}4H_2O$

atom	x	y	z	U_{eq}[a]
Ge(1)	$^1/_4$	0	$^1/_2$	0.0091
Al(1)	$^1/_4$	$^1/_2$	0	0.0055
O(1)	0.1412(4)	0.4202(3)	0.1422(4)	0.0147
Na(1)[b]	0.1460(6)	0.1460	0.1460	0.0277
O(2)	0.3753(7)	0.3753	0.3753	0.0305

[a] $U_{eq}(Å^2) = (U_1U_2U_3)^{1/2}$. [b] Fractional site occupancy = 0.75.

Table 7. Atomic Positional Parameters and U_{eq} Values for $Na_3(GaGeO_4)_3{\cdot}4H_2O$

atom	x	y	z	U_{eq}[a]
Ga(1)	$^1/_4$	0	$^1/_2$	0.0101
Ge(1)	$^1/_4$	$^1/_2$	0	0.0111
O(1)	0.1358(3)	0.1441(3)	0.4111(3)	0.0144
Na(1)[b]	0.1425(6)	0.1425	0.1425	0.0269
O(2)	0.3746(8)	0.3746	0.3746	0.0288

[a] $U_{eq}(Å^2) = (U_1U_2U_3)^{1/3}$. [b] Fractional site occupancy = 0.75.

Table 8. Atomic Positional Parameters and U_{iso} Values for $Na_3(GaSiO_4)_3{\cdot}4H_2O$

atom	x	y	l	U_{iso}[a]
Ga(1)	$^1/_4$	$^1/_2$	0	0.0107(6)
Si(1)	$^1/_4$	0	$^1/_2$	0.0018(8)
O(1)	0.1261(4)	0.4238(5)	0.1494(4)	0.016(2)
Na(1)[b]	0.1460(6)	0.1460	0.1460	0.036(4)
O(2)	0.3750(5)	0.3750	0.3750	0.002(4)

[a] U_{iso} in Å^2. [b] Fractional site occupancy = 0.75.

Table 9. Atomic Positional Parameters and U_{iso} Values for $Na_3(ZnAsO_4)_3{\cdot}4H_2O$

atom	x	y	z	U_{iso}[a]
Zn(1)	$^1/_4$	0	$^1/_2$	0.008(3)
As(1)	$^1/_4$	$^1/_2$	0	0.009(3)
O(1)	0.1488(5)	0.4022(5)	0.1232(5)	0.012(2)
Na(1)[b]	0.137(2)	0.137(2)	0.137(1)	0.014(4)
O(2)	0.3739(7)	0.3739(7)	0.3739(7)	0.020(3)
H(1)[c]	0.30(2)	0.337(6)	0.30(2)	0.04(2)
H(2)[c]	0.343(4)	0.466(4)	0.300(4)	0.06(2)

[a] U_{iso} in Å^2. [b] Fractional site occupancy = 0.75. [c] Fractional site occupancy = 0.333.

Table 10. Bond Distances (Å)/Angles (deg) for $Na_3(AlGeO_4)_3{\cdot}4H_2O$

Ge(1)–O(1)	1.746(4) × 4	Al(1)–O(1)	1.758(4) × 4
Na(1)–O(1)	2.459(6) × 3	Na(1)–O(2)	2.441(6) × 3
O(1)–Ge(1)–O(1)′	107.8(1)	O(1)–Ge(1)–O(1)′	112.8(2)
O(1)–Al(1)–O(1)′	107.9(1)	O(1)–Al(1)–O(1)′	112.6(2)
O(1)–Na(1)–O(1)′	91.8(3)	O(2)–Na(1)–O(1)	93.4(2)
O(2)–Na(1)–O(1)′	172.4(5)	O(2)′–Na(1)–O(1)	93.6(2)
O(2)–Na(1)–O(2)′	80.7(5)	Al(1)–O(1)–Ge(1)	129.6(2)
Na(1)–O(1)–Ge(1)	114.5(2)	Na(1)–O(1)–Al(1)	114.0(2)
Na(1)–O(2)–Na(1)′	98.6(4)		

Final atomic positional and equivalent isotropic thermal parameters for $Na_3(AlGeO_4)_3{\cdot}4H_2O$, $Na_3(GaGeO_4)_3{\cdot}4H_2O$, $Na_3(GaSiO_4)_3{\cdot}4H_2O$, and $Na_3(ZnAsO_4)_3{\cdot}4H_2O$ are listed in Tables 6–9, respectively. Selected bonds distance/angle data are presented in Tables 10 ($Na_3(AlGeO_4)_3{\cdot}4H_2O$), 11 ($Na_3(GaGeO_4)_3{\cdot}4H_2O$), 12 ($Na_3(GaSiO_4)_3{\cdot}4H_2O$), and 13 ($Na_3(ZnAsO_4)_3{\cdot}4H_2O$). AlGe–SOD, GaGe–SOD, GaSi–SOD, and ZnAs–SOD crystallize as typical sodalite frameworks with a fully-ordered alternating array of AlO_4/GeO_4, GaO_4/GeO_4, GaO_4/SiO_4, and ZnO_4/AsO_4 tetrahedra, respectively. The two T-atoms are on special positions (site symmetry $\bar{4}$) and the bridging oxygen atom is on a general position. The extra-framework configurations for each species are also similar: a defect-"cubane"-like $Na_3{\cdot}4OH_2$ cluster, occupying the β-cage. The 75% occupancy sodium cations (site symmetry .3.) occupy sites near the intercage 6-ring windows

Table 11. Bond Distances (Å)/Angles (deg) for $Na_3(GaGeO_4)_3 \cdot 4H_2O$

Ga(1)–O(1)	1.839(3) × 4	Ge(1)–O(1)	1.745(3) × 4
Na(1)–O(1)	2.420(6) × 3	Na(1)–O(2)	2.422(5) × 3
O(1)–Ga(1)–O(1)′	108.22(8)	O(1)–Ga(1)–O(1)′	112.0(2)
O(1)–Ge(1)–O(1)′	107.38(8)	O(1)–Ge(1)–O(1)′	113.7(2)
O(1)–Na(1)–O(1)′	91.1(3)	O(2)–Na(1)–O(1)	92.2(2)
O(2)–Na(1)–O(1)′	93.9(2)	O(2)′–Na(1)–O(1)	174.0(6)
O(2)–Na(1)–O(2)′	82.5(6)	Ge(1)–O(1)–Ga(1)	125.3(1)
Na(1)–O(1)–Ga(1)	114.6(1)	Na(1)–O(1)–Ge(1)	118.6(1)
Na(1)–O(2)–Na(1)′	98.6(6)		

Table 12. Bond Distances (Å)/Angles (deg) for $Na_3(GaSiO_4)_3 \cdot 4H_2O$

Ga(1)–O(1)	1.847(4) × 4	Si(1)–O(1)	1.581(3) × 4
Na(1)–O(1)	2.468(6) × 3	Na(1)–O(2)	2.417(6) × 3
O(1)–Ga(1)–O(1)′	107.1(2)	O(1)–Ga(1)–O(1)′	110.7(2)
O(1)–Si(1)–O(1)′	108.6(2)	O(1)–Si(1)–O(1)′	111.3(3)
O(1)–Na(1)–O(1)′	93.5(3)	O(2)–Na(1)–O(1)	90.4(2)
O(2)–Na(1)–O(1)′	170.7(4)	O(2)′–Na(1)–O(1)	94.8(2)
O(2)–Na(1)–O(2)′	80.9(4)	Ga(1)–O(1)–Si(1)	131.9(3)
Ga(1)–O(1)–Na(1)	108.2(2)	Si(1)–O(1)–Na(1)	118.9(2)
Na(1)–O(2)–Na(1)′	98.5(4)		

Table 13. Bond Distances (Å)/Angles (deg) for $Na_3(ZnAsO_4)_3 \cdot 4H_2O$

Zn(1)–O(1)	1.974(4) × 4	As(1)–O(1)	1.689(4) × 4
Na(1)–O(1)	2.40(2) × 3	Na(1)–O(2)	2.38(2) × 3
O(2)–H(1)	0.97(3)	O(2)–H(2)	1.11(4)
O(1)–Zn(1)–O(1)	109.7(2)	O(1)–As(1)–O(1)	107.0(2)
Zn(1)–O(1)–As(1)	121.1(3)	O(1)–Na(1)–O(1)	90.7(4)
O(2)–Na(1)–O(2)	85.0(5)		

and are three-coordinated to the framework oxygen atoms, and three-coordinated to oxygen atoms of water molecules, resulting in fairly-regular octahedral Na^+ coordination, as found for the aluminosilicate analog. Each water molecule oxygen atom is in contact with three sodium cation neighbors, resulting in pyramidal oxygen/sodium coordination (see Figure 5). The water proton positions were located in previous neutron diffraction studies on $Na_3(AlSiO_4)_3 \cdot 4H_2O$[25] and the before mentioned $Na_3(ZnAsO_4)_3 \cdot 4H_2O$ study.[18] In the ZnAs–SOD, significant H-bonding interaction is evident between one of the protons of the guest water molecule (H(2)) and the framework oxygen atom (O(1)). Inspection of the bond lengths indicates that the bond length between this proton and the oxygen atom of the water molecule (H(2)–O(2); d = 1.11(4) Å) is significantly longer than for the one associated with H(1) (d = 0.97(3) Å) (see Table 13).

For $Na_3(AlGeO_4)_3 \cdot 4H_2O$, bond distances are typical for the species concerned. The four equivalent Al–O distances (d = 1.746(4) Å) are in good accordance with the expected Al–O contact based upon ionic radii sums[26,27] of 1.75 Å. The Ge–O separation (d = 1.758(4) Å) also accords with the expected value of 1.76 Å. Another key parameter in defining tetrahedral-atom framework geometry is the T–O–T′ bond angle: for $Na_3(AlGeO_4)_3 \cdot 4H_2O$ this angle is 129.6(2)°, as compared to 132.6(3)° for AlSi–SOD. The sodium cation shows a typical octahedral bonding environment (d_{av} = 2.450(5) Å). The atomic parameters for $Na_3(GaGeO_4)_3 \cdot 4H_2O$ are also in accordance with previous studies: d(Ga–O) = 1.839(3) Å (ionic radii sum = 1.83 Å), d(Ge–O) = 1.745(3) Å, θ(Ga–O–Ge) = 125.3(2)°, d_{av}(Na–O) = 2.421(4) Å. As with all the analogs studied, the atomic parameters for $Na_3(GaSiO_4)_3 \cdot 4H_2O$ are in accordance with the studies mentioned above: d(Ga–O) = 1.847(4) Å, d(Si–O) = 1.581(3) Å (ionic radii sum = 1.61 Å), θ(Ga–O–Si) = 131.9(3)°, d_{av}(Na–O) = 2.468(6) Å. The atomic parameters for $Na_3(ZnAsO_4)_3 \cdot 4H_2O$ are also analogous with the other sodalite frameworks: d(Zn–O) = 1.974(4) Å, d(As–O) = 1.689(4) Å (ionic radii sum = 1.808 Å), θ(Zn–O–As) = 121.1(3)°, d_{av}(Na–O) = 2.40(2) Å.

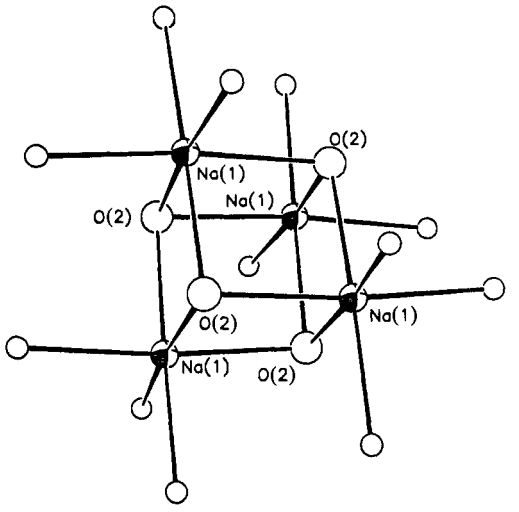

Figure 5. ORTEP figure of the defect-"cubane"-like $Na_3 \cdot 4OH_2$ cluster occupying the β-cage.

Thermogravimetric Analyses. The hydrated AlGe sodalite framework shows a distinct weight loss in air of approximately 12.3%, at an onset temperature of 300 °C. Under vacuum the onset temperature increases slightly to 320 °C. The DSC data show a corresponding exotherm associated with the dehydration process. Calculated weight loss for the hydrated sodalite, of 11.4%, versus the basic hydroxy sodalite of 13.25% indicates that the system does not contain the intercage hydroxide ion.

The hydrated GaGe sodalite framework shows a sharp weight loss in air of 10.5%, at an onset temperature of 300 °C. Under vacuum, the onset temperature slightly increases to 320 °C, at which point the DSC data show a corresponding exotherm associated with the dehydration process. Calculated weight loss for the hydrated sodalite, of 9.56%, versus the basic hydroxy sodalite, of 11.11%, indicates that the framework does not contain a hydroxide ion.

The hydrated GaSi sodalite framework shows a gradual weight loss in air of approximately 11.2%, describing a fully hydrated sodalite losing 8 water molecules per unit cell (calculated value 11.51%) instead of a partially-basic hydroxy sodalite losing 9 water molecules per unit cell (12.16%). In conjunction with crystallographic refinement studies to determine the exact water content, thermal studies under vacuum were performed. Though the same results were obtained in terms of percentage weight loss, the onset temperature (under vacuum conditions) for water loss increased from 100 to 300 °C, at which point the DSC data also show a corresponding exotherm with the single dehydration process.

The hydroxy hydrated AlSi sodalite framework shows a gradual two part weight loss in air totaling approximately 8.1%, describing the loss of an average of 1.72 water molecules and one $O_{0.5}H$ group per β-cage. The hydrated AlSi sodalite framework shows a gradual weight loss of approximately 14.5% due to the loss of 4 water molecules per β-cage, or 8 water molecules per unit cell.

***In Situ* Variable-Temperature X-ray Powder Diffraction Studies.** In order to further elucidate the discrepancies between the crystallographic description of the sodalite water content and the thermogravimetric data, an *in situ* variable-temperature X-ray powder diffraction study was performed with the GaSi–SOD powder. The analysis of the change in unit cell versus temperature showed that the material can stay highly crystalline until over 600 °C (see Figure 6). The unit cell value remains constant (within experimental error) until approximately 175 °C, after which point there is a sharp increase in unit cell size until approximately 450 °C. It is at this point that there seems to be a plateau; the unit cell size remains constant until 600 °C. It is

(26) Shannon, R. D.; Prewitt, C. T. *Acta Crystallogr.* **1969**, *B25*, 925.
(27) Shannon, R. D.; Prewitt, C. T. *Acta Crystallogr.* **1976**, *A32*, 751.

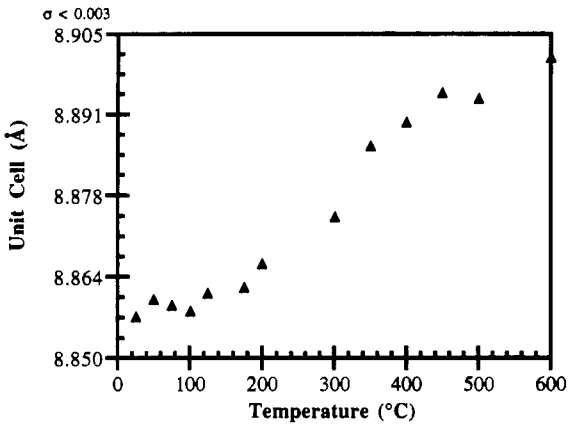

Figure 6. *In situ* variable-temperature powder X-ray diffraction study of GaSi–SOD: Plot of the unit cell versus temperature.

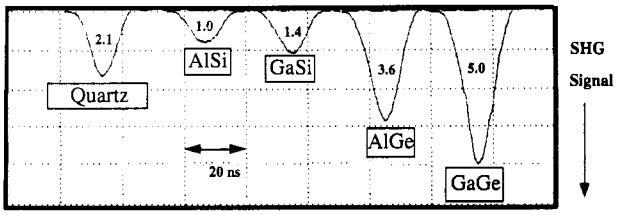

Figure 7. Plots of the SHG responses of AlSi–SOD, GaSi–SOD, AlGe–SOD, and GaGe–SOD as compared to quartz.

at approximately 650 °C (still under a vacuum of 1×10^{-6} Torr) that the sodalite structure transforms hexagonally (a = 8.784(4) Å, c = 8.419(6) Å), as witnessed with the ZnAs–SOD structure (a = 9.005(2) Å, c = 8.161(2) Å).[8]

The increase in unit cell size, while still cubic, is attributed to the removal of the water molecules from the cage. The water is bound to the sodium cations in a tight cubane-type structure, with its protons hydrogen-bonding to the oxygen atoms of the framework (see above). As the water is removed through dehydration, the framework is allowed to expand, the sodium cations move toward the 6-ring windows and the unit cell increases. The vacuum process seems to aid in the water removal and add stability to the framework by alleviating any pressure due to steaming of the water during dehydration. This is an explanation for the difference in temperatures of dehydration between the TGA data at atmospheric pressure and the data under vacuum.

Second Harmonic Generation Measurements. Results showed that the SHG intensities for isomorphous structures increase when framework atoms going down the periodic table are added. In spite of the fact that a universal theory on all possible contributions to the SHG efficiency for particular crystal symmetry has not been yet developed, there is a general agreement that an increase in bond polarizabilities and the decrease in magnitude of the band gap contribute to an overall increase in SHG. Our experimental observations are in agreement with the theory that bond polarizabilities increase with heavier framework ion substitution. Furthermore, our results show that by altering the framework composition from $AlSiO_4$ to the $GaGeO_4$, we observe a decrease in the band gap; the AlSi–SOD has an $E_g > 6$ eV while the GaGe–SOD has an $E_g \approx 4.6$ eV.[28] Because the $Na_3[\,](ABO_4)_3{\cdot}4H_2O$ sodalites all crystallize in the common space group $P\bar{4}3n$, and since there is an assumption that sizes of the crystallites were similar, the experimental results provided the information about the ratio of the second-order nonlinear susceptibilities for these analogs: AlSi–SOD:GaSi–SOD:AlGe–SOD:GaGe–SOD = 1:1.4:3.7:5.2 (see Figure 7).

(28) Srdanov, V. I.; Stucky, G. D. Unpublished results, 1992.

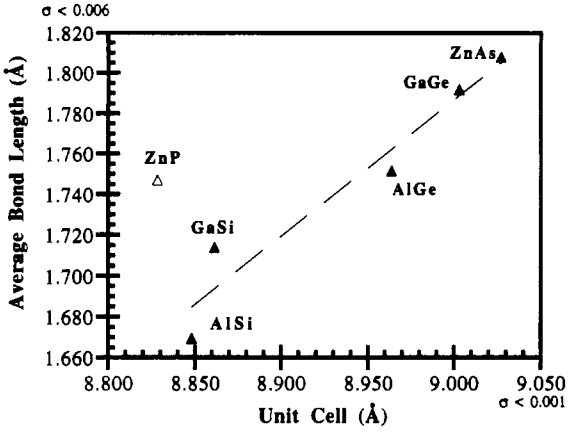

Figure 8. Plot of unit cell sizes of sodalite analogs versus average bond lengths of T–O and T′–O.

Table 14. Data for $Na_3(ABO_4)_3{\cdot}4H_2O$ Compounds

composn	a (Å)	θ(T–O–T) (deg)	area (Å²)	δ(Na ring) (Å)
$Na_3(AlSiO_4)_3{\cdot}4H_2O$	8.848(1)	136.2(3)	5.750	1.53(1)
$Na_3(GaSiO_4)_3{\cdot}4H_2O$	8.8614(2)	131.9(3)	5.599	1.60(4)
$Na_3(AlGeO_4)_3{\cdot}4H_2O$	8.964(1)	129.6(2)	5.399	1.61(1)
$Na_3(ZnPO_4)_3{\cdot}4H_2O$	8.8281(1)	126.1(3)	5.280	1.66(1)
$Na_3(GaGeO_4)_3{\cdot}4H_2O$	9.003(1)	125.5(2)	5.172	1.68(1)
$Na_3(ZnAsO_4)_3{\cdot}4H_2O$	9.0273(1)	123.8(3)	4.741	1.73(1)

Summary

The initial theory about the sodalite tetrahedral atom substitution was that, with increasing T-atom ionic radii, increased sodalite cages (larger cages and larger unit cells) would be synthesized. However, results quickly indicated that with the presence of the intercage $Na_3{\cdot}4OH_2$ cubane structure, there is very little variation in the unit cell. The framework compensates for the increase in T-atom size by decreasing the T–O–T′ angle. This angle decrease seems to be facilitated by a "pulling" of the framework oxygen atom involved in hydrogen-bonding to the intercage water molecules. Furthermore, a study of the distance of the sodium cations from the famework 6-ring indicates that it remains toward the center of the cage in the cubane structure but migrates toward the ring opening in the electride and dehydrated phases. Not surprisingly, these sodalites have a dramatic increase in unit cell size and also find the sodium cation, which is no longer bound by the water molecules, almost exactly in the face of the 6-ring (as measured by δ, the distance of Na^+ from the plane of the metal atoms in the 6-ring) (see Table 14).

There are interesting progressive trends in cell sizes and ionic radii that the various analogs follow that indicate an overall consistency to the sodalite framework. When the unit cell sizes of the analog frameworks are compared (in Å) versus half the sum of the T–O and T′–O bond lengths (in Å), a linear relationship is found (see Figure 8). However, this is only if the Zn/P (ZnP–SOD)[18] analog is discarded, as it does not follow the overriding trend. The same result is found if the T–O–T′ bond angle (deg) is plotted versus half the sum of the T–O and T′–O bond lengths, except for the Zn/P analog (see Figure 9). Because of the discrepancy with the zincophosphate sodalite, a theory of diminished stability in the framework due to both a deviation from mean bond lengths and from mean O–T–O bond angles was studied. In this system (with the short P–O bond length) the average T–O bond length is comparable to the other sodalite frameworks T–O lengths, yet the actual difference of the bond length with the average is the greatest (see Table 15). It is possible that the large difference (Δ(Å)) between the Zn–O and P–O bond lengths actually forms a more unstable, strained sodalite framework which is highly condensed to accommodate the alternating short and long bonds. It follows that the sodalite

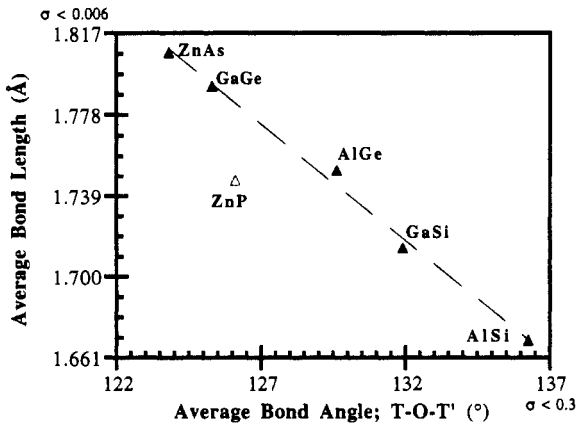

Figure 9. Plot of T–O–T′ bond angle of various sodalite analogs versus the average of the T–O and T′–O bond lengths.

Table 15. Bond Length and Angle Comparisons for $Na_3[\,](ABO_4)_3{\cdot}4H_2O$

sodalite	T–O	d_{T-O} (Å)	d_{av} (Å)	Δ (Å)	O–T–O_{av} (deg)	θ_{av} (deg)	Δ (deg)
AlSi	Al–O	1.758	1.6695	0.0885	109.7	110.0	0.30
	Si–O	1.581			110.3		
AlGe	Ge–O	1.746	1.752	0.006	110.25	110.28	0.025
	Al–O	1.758			110.30		
GaSi	Ga–O	1.847	1.714	0.133	108.9	109.42	0.525
	Si–O	1.581			109.95		
GaGe	Ga–O	1.839	1.792	0.047	110.11	110.32	0.215
	Ge–O	1.745			110.54		
ZnAs	Zn–O	1.946	1.808	0.138	109.6	110.2	0.60
	As–O	1.670			110.8		
ZnP	Zn–O	1.964	1.747	0.216	107.90	109.18	1.285
	P–O	1.531			110.47		

frameworks built from T-atoms of similar ionic radii will be more stable. To test this theory, a study of the deviation from the mean O–T–O bond angle was undertaken from the crystallographic data. For all the sodalite analogs, except ZnP–SOD, the bond angles are relatively the same, with deviations ≤ 0.60°. However, there is an enhanced difference in the ZnP system (Δ ≈ 1.285°), producing an alternation of wide and narrow angles, and the predicted highly distorted sodalite framework (see Table 15).

A recent crystallographic study of $Na_4[e^-](AlSiO_4)_3$ (Black–SOD)[29,30] shows this framework to also follow the trends of the unit cell and δ with the aluminosilicates and the other analogs studied. Furthermore, the Black–SOD behaves as would be predicated with the hydrated and the dehydrated aluminosilicates. Because there are no water molecules in the cage to constrict the framework, the Black–SOD has an increased unit cell size, enlarged T–O–T′ angles, increased 6-ring area, and a longer δ length (sodium is not restricted by the cubane structure) than AlSi–SOD, yet smaller than the expanded dehydrated $Na_3(AlSiO_4)_3$.

It is important to note that the framework T-atoms with the smallest radii sum (AlSi–SOD) has the largest pore opening and the largest radii sum (ZnAs–SOD) leads to the smallest pore opening, with the other analogs following the trend (see Table 14). It is clear that T-atoms can in fact decrease pore diffusivity, as exhibited through the thermal property studies. The aluminosilicate sodalite loses water weight very gradually after the onset temperature of 100 °C (in air). This gradual transition allows for the water to break the cubane structure and leave the sodalite cage under nonstrenuous conditions. The resulting cell

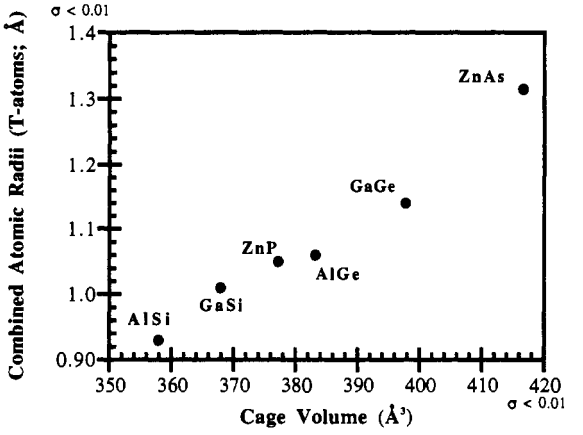

Figure 10. Plot of approximate sodalite cage volumes versus combined atomic radii of tetrahedral atoms.

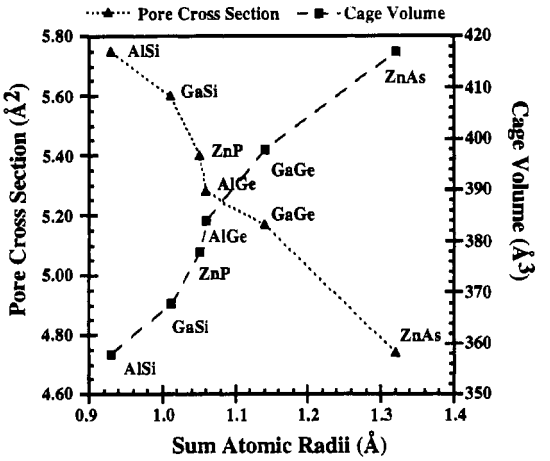

Figure 11. Plot of the inverse relationship between the pore cross section (Å²) and cage volume (Å³) versus the sum of the atomic radii (Å) of the T-atoms for the SOD framework analogs.

is free to expand without transforming into a collapsed structure. This is in contrast to the Zn/P and Zn/As analogs. These frameworks dehydrate very quickly, with a sharp transitional weight loss at 145 and 175 °C, respectively. The water is not able to leave the cage gradually. Instead it immediately is removed, causing the frameworks to collapse into a hexagonal, stuffed-tridymite analog (see below).[8] The remaining $Na_3[\,](ABO_4)_3{\cdot}4H_2O$ structures have thermal characteristics in between these two extremes. The gallogermanate analog is the least stable to thermal degradation. It has a somewhat sharp thermal transition and also collapses to a hexagonal phase, when heated in air. The gallosilicate sodalite will collapse into the hexagonal phase when heated in air but will retain the cubic phase until approximately 650 °C, when heated slowly in vacuum. The *in situ* data also indicate the possibility of enhanced thermal stability at approximately 450 °C. This is of interest with future studies of loading this dehydrated material with one further sodium cation and a solvated electron to form $Na_4[e^-](GaSiO_4)_3$. The aluminogermanate analog has a much more gradual dehydration process. $Na_4[e^-](GaGeO_4)_3$ is then also of interest in future solvated electron studies.

The *larger* T-atoms in the framework do not lead to greatly increased unit cell sizes and actually restrict the 6-ring openings and diffusion rates, but they do *enlarge* the volume of the sodalite cage. The cage volume may be approximated for each of the analogs by determining a fixed cubic area in the cage (with each corner of the cube being the center point of the three oxygen atoms pointing into the cell). Calculations show that the largest framework T-atoms, ZnAs–SOD (measured by combined atomic radii), produce the largest cube volume. The cube volumes of the analog cages also decrease in a linear fashion as the T-atoms

(29) Nenoff, T. M. Ph.D. Dissertation (Chemistry), University of California, Santa Barbara, CA 93106, 1993.
(30) Srdanov, V. I.; Nenoff, T. M.; Monnier, A.; Stucky, G. D. Manuscript in preparation.
(31) Johnson, C. K. *Report ORNL-5138*; Oak Ridge National Laboratory: Oak Ridge, TN 37830, 1976; with local modifications.

decrease in combined size, with the smallest T-atoms (AlSi–SOD) having the smallest calculated volume (see Figure 10).

This paper explicitly details our ability to synthesize a wide variety of analogs to the $Na_3[\ ](ABO_4)_3{\cdot}4H_2O$ sodalite framework and also our ability to dehydrate these sieves while retaining the structure. We have synthesized high-quality single crystals of the GaGe–SOD and AlGe–SOD systems, so as to be able to correctly solve space groups by differentiating between atoms with similar electron density by X-ray diffraction. Though a large size range of tetrahedral atoms was used in the synthesis with the hope of synthesizing larger pore opening molecular sieves, we have shown that the framework unit cell does not change significantly. In contrast, the inter-cage pore size *decreases* with increasing T-atom size so that dehydration tends to be more difficult. However, calculations of a cube area inside each of the sodalite cages do show that, by increasing the size of the T-atoms in the framework, we are able to *increase* the volume of the cage (see Figure 11). Various thermogravimetric methods and *in situ* variable-temperature X-ray studies have determined that many of the sodalite analogs are eligible for dehydration, and subsequent metal loadings, to form the $Na_4[e^-](ABO_4)_3$ framework. We believe that future Wigner lattice studies will provide interesting results in the variation of electron structures among these sodalite framework analogs.

Acknowledgment. We thank the Office of Naval Research and the National Science Foundation (QUEST, DMR No. 91-20007) for their financial support. We also thank Andrew Saab for providing the single crystal of hydroxy hydrated aluminosilicate sodalite.

Supplementary Material Available: Listings of the crystallographic parameters and anisotropic thermal parameters for $Na_3(AlGeO_4)_3{\cdot}4H_2O$ and $Na_3(GaGeO_4)_3{\cdot}4H_2O$ and listings of the crystallographic parameters for $Na_3(GaSiO_4)_3{\cdot}4H_2O$ and $Na_3(ZnAsO_4)_3{\cdot}4H_2O$ (5 pages). Ordering information is given on any current masthead page.